Linearity of Sequential Molecular Signals in Turbulent Diffusion Channels

Mahmoud Abbaszadeh[1], H. Birkan Yilmaz[2], Peter J. Thomas[1], Weisi Guo[1,*]
[1]School of Engineering, University of Warwick, Coventry, United Kingdom
[2]Dept. of Network Engineering, Polytechnic University of Catalonia, 08034, Barcelona, Spain.

***Abstract*—Molecular communication underpins biological system coordination across multiple spatial and temporal scales. Whilst significant research has focused on micro-scale diffusion dominated channels, far less is understood of macro-scale flow dominated channels. The latter introduces complex fluid dynamic forces, one of which is turbulent diffusion. Molecular Communication via Turbulent Diffusion (MCvTD) more accurately reflects realistic molecular channels in both pheromone signaling and chemical engineering. Current literature assumes linear combining between sequential molecular signals, but this assumption may not hold when turbulence is introduced. Here, we use computational fluid dynamics (CFD) simulation to show that sequential MCvTD signals do indeed linearly combine. This is a non-trivial and non-intuitive result and our conclusion allows the research field to leverage on existing linear combining signal analysis. To ensure robustness of our results, we test for the received signal strength and Inter-Symbol-Interference (ISI) under different concentrations, co-flow rate, and the information sequence. Also, we introduce a basis for the channel model in a way that for any k sequential signals in which $k \geq 4$, by understanding the $1 \leq k \leq 3$ signals and the last signal, we can represent the other signals. We expect these results to be useful to both molecular communication and biological signaling researchers.**

***Index Terms*—molecular communication, turbulence, CFD.**

I. Introduction

Molecular Communication (MC) exists in various forms in nature to enable simple components (e.g. cells) to be connected and to coordinate complex system-level actions. Inspired by this, some recent applications of MC has provided new growth pathways in nano-medicine, heavy industrial sensing, and secure communications [1], [2]. In such applied MC systems, the information is encoded to a property of the Messenger Molecules (MMs), then the molecules propagate through the channel and when they are captured by a receiver, the decoding process takes place to recognize the information [3]. What is important here is how different emissions of molecules can interfere with each other when there is a sequential release of molecules [4]–[6].

In general, the MC application environment can be classified into two broad regimes. In the micro- to nano-scale regime, mass diffusion dominates propagation and the vast majority of current literature [7]. For a mass diffusion-dominated MC channel, we assume that the molecular trajectories are independent and identically distributed, which gives rise to linear combining at any given point. As such, this makes signal and ISI analysis linear [8], [9]. Current mass diffusion dominated studies can be characterized by a low Péclet number, whereby the relative value of kinematic viscosity is low compared to mass diffusivity. This is particularly the case for cell signaling and small blood vessel transport.

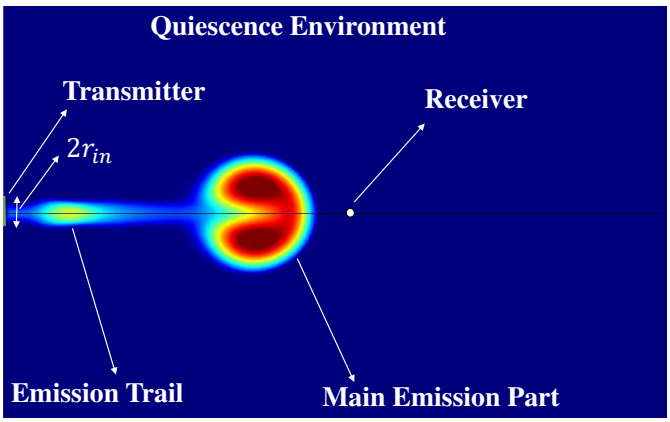

Fig. 1. Schematic of the system model showing the quiescence environment, the transmitter, the receiver, and the emitted molecules.

In this paper, we consider the turbulent diffusion regime (MCvTD) whereby the Péclet number is large. In this case, when flow (co-flow) dominates the propagation mechanism, turbulence can become a dominate factor (high Reynolds number) and the analysis becomes non-trivial. This is typical in pheromone communications between animals and plants [10], underwater signaling, and in heavy industry applications (e.g. chemical plants). In past laboratory experiments [11], [12], preliminary findings indicate potential non-linearity, but the causal mechanisms are not well understood [13]. Later work have attempted to both characterize non-linear turbulent effects in a stationary environment [10] and embed information optimally in turbulent structures [14].

To continue this line of research, we employed the CFD module in COMSOL Multiphysics Finite Element software to simulate and analyse the degree of non-linearity in the turbulent diffusion propagation for sequential signal pulses. Up to our knowledge, this is the first study that explicitly investigates the non-linearity aspects of the turbulence and

The work of M. Abbaszadeh, P. J. Thomas, and W. Guo is funded by the US AFOSR grant FA9550-17-1-0056. The work of H. B. Yilmaz is supported by the Government of Catalonia's Secretariat for Universities and Research via the Beatriu de Pinos postdoctoral programme. *Corresponding Author: weisi.guo@warwick.ac.uk

TABLE I
SIMULATION PARAMETERS

Variable	Value
Maximum Injection Velocity, u_{in}	$2\,\mathrm{m/s}$ at $t=0$
Kinematic Viscosity of water, ν	$1\times10^{-6}\,\mathrm{m^2/s}$
Density of water, ρ	$1000\,\mathrm{kg/m^3}$
Transmit Concentration, c_0	$1\,\mathrm{mol/m^3}$
Pulse Width, T_0	$0.7\,\mathrm{s}$
Radius of the injector (r_{in})	$10\,\mathrm{cm}$
Distance Between TX and RX, $d_{Tx,Rx}$	$60\times r_{in}$
Simulation Space Length	$200\,r_{in}$
Simulation Space Width	$60\,r_{in}$

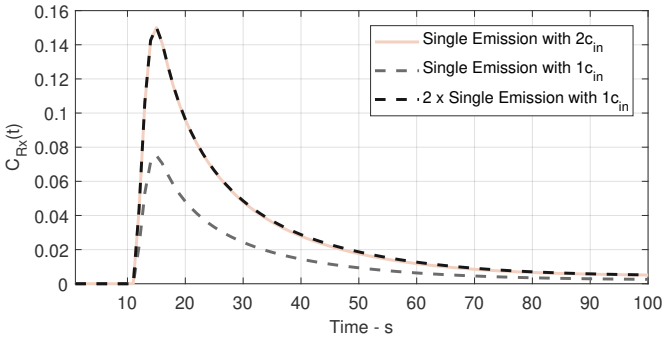

Fig. 2. Channel response for a single emission.

attempts to create a channel model.

The rest of the paper is organized as follows. In section II, the channel configuration and the turbulence equations has been introduced. Section III, accounts for two different scenarios of non-linearity analysis and in section IV, the interference modeling of the TDMC channel has been discussed. Finally, we wrap up the main contribution in section V and we present possible avenues for extending the current study.

II. SYSTEM MODEL

Molecular communication via turbulent diffusion system is at least composed of a transmitter node, environment, the MMs, and the receiver node (see Fig. 1). We consider turbulent diffusion as the carrier mechanism since it is the most realistic model for real life applications. In Turbulent diffusion, the effects of the molecular diffusion are negligible and the eddy diffusivity effects are responsible for transporting the MMs.

A. Channel Configuration

The system model is comprise of an injector which releases the water molecules into the quiescence aqueous environment with the velocity of u_{in} (see Fig. 1). The radius of the injector is r_{in}, and in order to simulate the motion of the injector piston, a hyperbolic function is defined at the inlet boundary. The flow domain is $10\times6\,\mathrm{m}^2$, and the lateral boundaries are $60\times r_{in}$ far from the transmitter and the outlet is located $200\times r_{in}$ away from the transmitter, so their effects on the flow field and emitted molecules are negligible. The distance between the transmitter (TX) and the receiver (RX) is considered as $60\times r_{in}$, and the concentration of the molecules are measured at the observing receiver. It is noteworthy that during the propagation of the molecules the main deriving process is governed by the Turbulent diffusion. The properties of the water and the other system parameters are given in Table I.

B. Advection-Diffusion Dynamics with RANS Equations

In order to obtain the concentration of the emitted molecules in the environment, we need to solve the advection-diffusion equation.

$$\frac{\partial c}{\partial t}=\nabla\cdot(D_\varepsilon\nabla c)-\nabla\cdot(\vec{v}c) \tag{1}$$

where c is the concentration and D_ε is the eddy diffusivity coefficient of the water molecules. c_0 is the amount of the molecules which are released into the channel at $t=0$, and v is the velocity field of the environment flow. Generally, there are two restrictions in solving (1). First of all, $\vec{v}$ is a function of the space and time which means that in any arbitrarily location and time, the velocity components should be calculated and substituted in (1) in order to find concentration distribution. In literature [15], this restriction has been ignored and they considered the velocity field constant spatially to find a closed-form relation for the concentration distribution. Secondly, the eddy diffusivity, D_ε, will be changed as the messenger molecules (MMs) go far away from the transmitter and it is not isotropic. In literature [3], the eddy diffusivity mostly has been considered isotropic which means that the information particles in the channel can be dispersed in any directions equivalently whilst this assumption is not accurate due to the essence of the turbulent flow [16].

Based on the aforesaid restrictions, considering anisotropic velocity and eddy diffusivity and also, considering time-variant velocity simultaneously makes the problem complicated and finding a closed-form solution is almost impossible. In order to address the foregoing problem, the velocity distribution should be obtained and employed in (1). One of the scheme to obtain the velocity distribution is using the numerical packages to simulate the flow field and solve the **Reynolds-Average-Navier-Stokes (RANS)** equations [16]. The key characteristic of the numerical packages like COMSOL Multiphysics is that they solved RANS equations with mass transport equation (1) simultaneously and it considers the effects of eddies on transporting the molecules from TX to RX.

$$c\overline{u}_j\frac{\partial\overline{u}_i}{\partial x_j}=c\overline{f}_i+\frac{\partial}{\partial x_j}\left[-\overline{p}\delta_{ij}+\mu\left(\frac{\partial\overline{u}_i}{\partial x_j}+\frac{\partial\overline{u}_j}{\partial x_i}\right)-c\overline{u_i'u_j'}\right] \tag{2}$$

where c represents density or concentration which depends on a number of pressure, velocity, and sheer stress gradients. μ is dynamic viscosity of the fluid, and $c\overline{u}_j\frac{\partial\overline{u}_i}{\partial x_j}$ represents the change in mean momentum of fluid element due to the unsteadiness in the mean flow and the convection by the mean flow. This is balanced by the mean body force $\overline{f}_i$, the isotropic stress from the pressure field $\overline{p}\delta_{ij}$, the viscous stresses, and apparent stress $-c\overline{u_i'u_j'}$ owing to the fluctuating velocity field (Reynolds stress). Whilst there are statistical

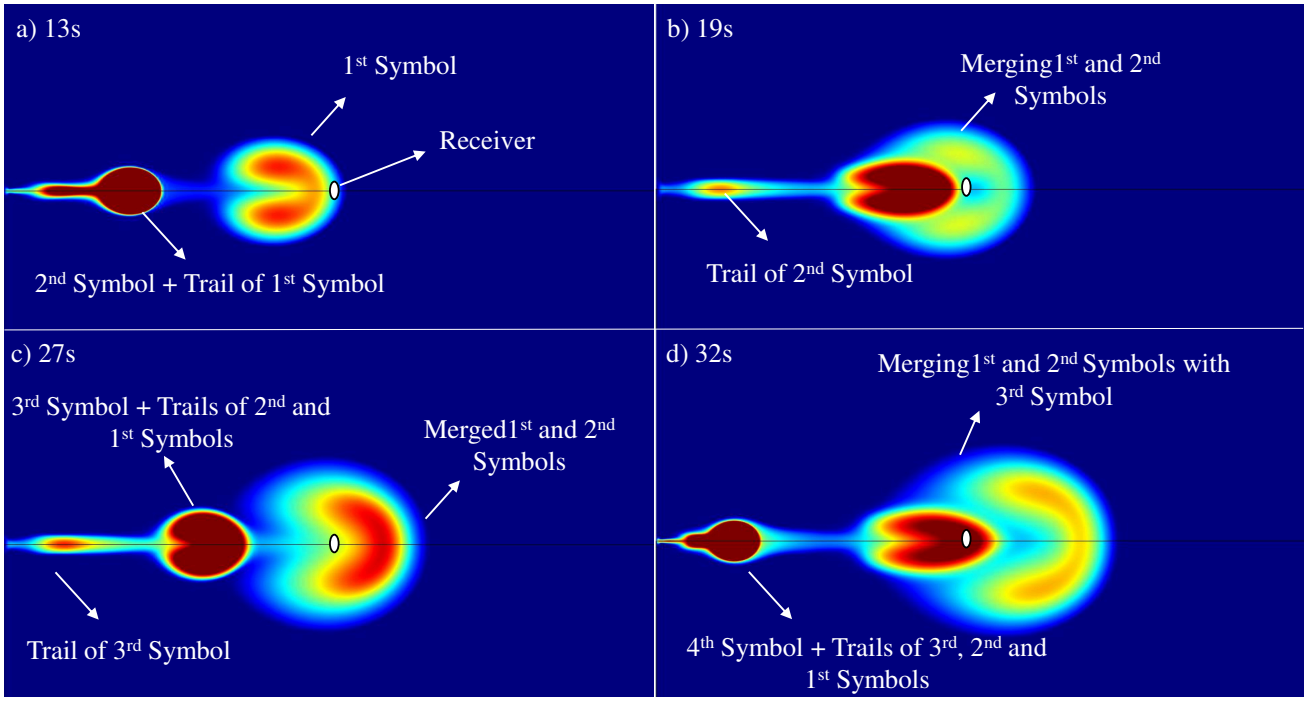

Fig. 3. Snapshots of the environment and the emitted molecules at different time instances for consecutive emissions. New emissions sweep the trails of the previous emissions.

approximate solutions in the form of eddy diffusivity, general tractability is still a challenge for modeling turbulent diffusion and that is why finite-element simulation is used.

III. Non-Linearity Analysis

The non-linearity of the molecular communication via turbulent diffusion channel is investigated with two scenarios: single emission and consecutive emissions.

A. Scenario with a Single Emission

In this scenario, at first we release water molecules with the concentration of c_{in} and in the second case, we emit $2 \times c_{in}$ concentration. Then, we double the observed concentration for the c_{in} emission and finally compare them with the $2 \times c_{in}$ concentration. In Fig. 2, time versus the measured concentration is shown. Output of the CFD simulator shows that the channel impulse response has the multiplicative property, which holds for infinitely many different cases with the same Reynolds number due to the non-dimensional solution.

B. Scenario with Consecutive Emissions

Sequential emissions of marked water molecule types are released to see the channel response of the n-th emission. In Fig. 3-a, we can see that the second emission sweeps the tail of the first emission and this behaviour is also seen in other subplots of the Fig. 3. The outcome of this behaviour is that some of the emitted molecules reach to the receiver lately and we have two or more peaks in the concentration profile at the receiver for the same molecule type (see Fig. 4). It should be mentioned that when we have only one emission like Fig. 2, we cannot observe the second and smaller peak as far as there is no other emission afterward that sweeps the trail of the previous emission. If there is no successive emissions that pushes the trail, the trail of the emission does not meet the receiver and remains in the environment (see Fig. 1).

In Fig. 4, time versus the received concentration is shown for the scenarios without and with co-flow. First critical observation is that there are four different classes of emissions in terms of channel response: first, second, last, and the rest of the emissions. First emission is different than the other emissions since the environment is quiescence and the first emission should overcome a higher drag force compared to the other emissions. The concentration at the receiver due to the first emission has two significant modes: the main and the trail parts (see Fig. 3 for contour plots for sequential emissions). After the first emission, the effect due to the trail decreases. Please also note that the effect due to trail decreases when there is a co-flow in the environment. Second emission is unique (i.e., it has higher peak value compared to other emissions) since it experiences less drag force compared to the first emission and most of the molecules can easily go through the environment. Also, the second emission is more compact when it meets the receiver compared to the other emissions. By comparing the Fig. 3-b and Figs. 3-c and -d, it is visible that the second emission is more compact than the third fourth emissions and as a result, the concentration of the molecules in second emission is more than the others. The last emission has different characteristics since there is no other

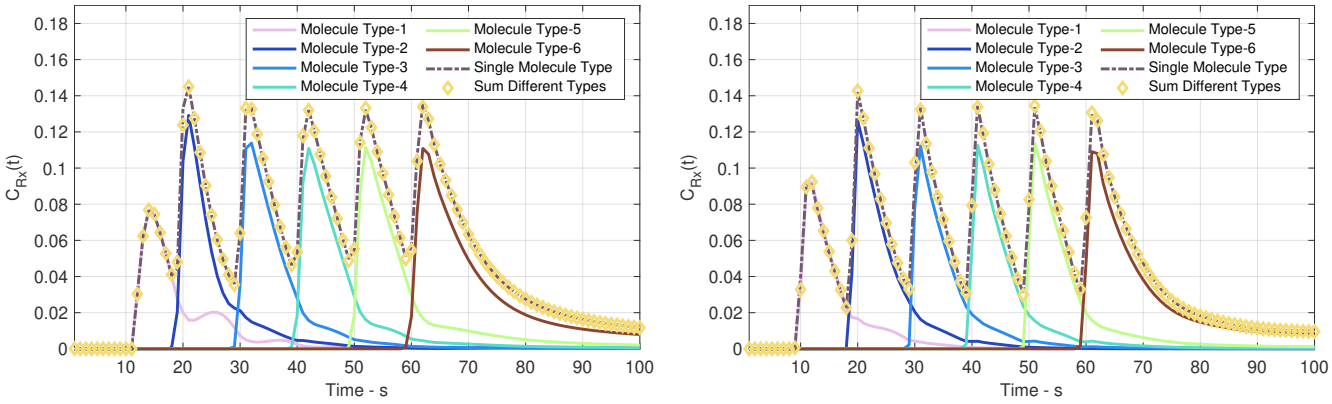

(a) $u_{co} = 0\,\mathrm{m/s}$ (b) $u_{co} = 0.02\,\mathrm{m/s}$

Fig. 4. Received concentration for six consecutive emissions. Molecule types are changed for distinguishing the effect of each emission. Scenarios without co-flow (a) and with co-flow (b) are considered. Red dashed curve corresponds to emission of single type molecule and the blue dashed curve corresponds to sum of six consecutive emissions with different molecule types.

following emission that is pushing off the molecules. The rest of the emissions (i.e., the third, fourth, and the fifth for the six emission scenario in Fig. 4) have similar structure.

In Fig. 4, we also observe that the sum of the six channel responses due to the sequential emissions gives nearly the same channel response when a single molecule is utilized. This additive property enables us to model the received signal (including interference), which will be detailed in the following section.

IV. Interference Modeling

Due to the additive property, we can introduce the channel model by considering the summation of the effect of sequential emissions. For this purpose, we use a model function for the received signal at a given point (x, y) with some control coefficients as follows:

$$c^{\mathrm{mdl}}(t|x,y) = \begin{cases} b_1 \frac{\sqrt{x^2+y^2}}{t^{b_2}} e^{-b_3 \frac{x^2+y^2}{t}} & \text{for } t > 0 \\ 0 & \text{otherwise} \end{cases} \quad (3)$$

where b_1, b_2, and b_3 are fitting parameters. The model function in (3) has the similar structure with the diffusion equation in 2D environment [17]. After we run simulations with COMSOL, we fitted the received signal classes/types with (3) and obtained the fitting parameters for each class.

Please note that, we observe four different classes of received signal patterns (see Fig. 4). We left the first emission as is (i.e., we used the empirical result c_1^{emp}) and fitted the other three classes and obtained $c_2^{\mathrm{mdl}}(t)$, $c_{\mathrm{last}}^{\mathrm{mdl}}(t)$, and $c_{\mathrm{mid}}^{\mathrm{mdl}}(t)$. Hence, the set $\mathscr{B}_c = \{c_1^{\mathrm{emp}}(t),\, c_2^{\mathrm{mdl}}(t),\, c_{\mathrm{mid}}^{\mathrm{mdl}}(t),\, c_{\mathrm{last}}^{\mathrm{mdl}}(t)\}$ forms a basis for our modeling. After obtaining the basis $\mathscr{B}_c$, for a case with K emissions in T_s-long symbol slots ($K \geq 4$), the received signal is given in (4).

Please note that, the model for the received signal is defined as a piece-wise function in which the cases are determined according to the time slot. In (4), most complicated case with at least four emissions is given, similarly lower number of emissions can be modeled with omitting the middle terms. For example, if we had only two emissions we should be considering $c_1^{\mathrm{emp}}(t)$ and $c_{\mathrm{last}}^{\mathrm{mdl}}(t)$.

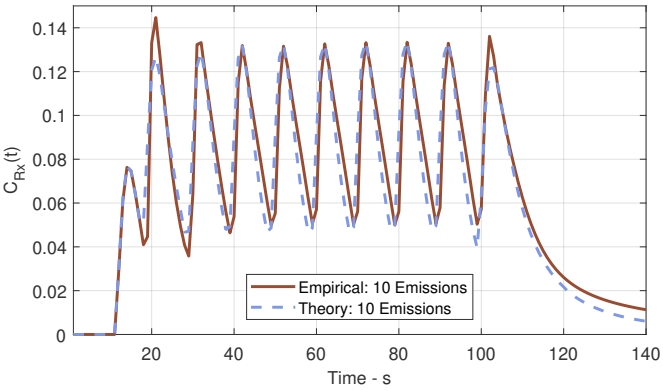

Fig. 5. Empirical and theoretical received concentration for 10 sequential emissions. Theoretical received signal is obtained by using the fitted base functions and (4).

In Fig. 5, empirical and theoretical received signals are shown for a case with 10 sequential emissions. Considering $\mathscr{B}_c$ enables us to model the received signal that includes interference. It can be clearly seen that the theoretical $C_{\mathrm{Rx}}(t)$ in (4) that is utilizing $c_1^{\mathrm{emp}}(t)$, $c_1^{\mathrm{emp}}(t)$, $c_{\mathrm{mid}}^{\mathrm{emp}}(t)$, and $c_{\mathrm{last}}^{\mathrm{mdl}}(t)$ is capable of modeling the received signal for the analyzed system. By having this model in hand, we can consider the interference effect of any number of sequential emissions.

To analyze the effect of interference, we first define signal-to-interference ratio (SIR_n) for a given ISI window length (i.e., the number of previous emissions that is considered for the interference) as follows:

$$C_{\text{Rx}}(t) = \begin{cases} c_1^{\text{emp}}(t) & \text{If } t \in [0, T_s) \\ c_1^{\text{emp}}(t) + c_2^{\text{mdl}}(t - T_s) & \text{If } t \in [T_s, 2\,T_s) \\ c_1^{\text{emp}}(t) + c_2^{\text{mdl}}(t - T_s) + \sum_{i=0}^{j-2} c_{\text{mid}}^{\text{mdl}}(t - (j-i)T_s) & \text{If } t \in [j\,T_s, (j+1)\,T_s) \text{ for } 2 \le j \le K-2 \\ c_1^{\text{emp}}(t) + c_2^{\text{mdl}}(t - T_s) + \sum_{i=1}^{j-2} c_{\text{mid}}^{\text{mdl}}(t - (j-i)T_s) + c_{\text{last}}^{\text{mdl}}(t - (K-1)T_s) & \text{If } t \in [(K-1)\,T_s, K\,T_s) \end{cases} \quad (4)$$

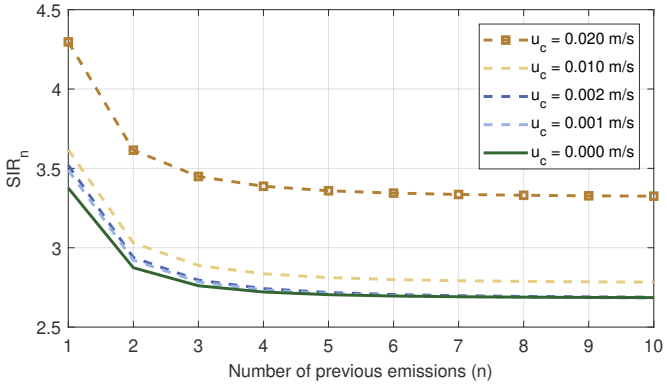

Fig. 6. SIR versus the number of previous emissions with different co-flow velocities.

$$\text{SIR}_n = \frac{\int_0^{T_s} C_{\text{Rx}}(t)\,dt}{\int_{T_s}^{(n+1)\,T_s} C_{\text{Rx}}(t)\,dt}. \quad (5)$$

We also introduced different co-flows into the environment and analyzed the effect of interference under different system conditions. For different system conditions we obtained basis $\mathscr{B}_c$ and evaluated SIR_n via theoretical model for different ISI window lengths to see the significant ISI window length.

In Fig. 6, ISI window length versus SIR_n values are plotted for different co-flow cases. Case without co-flow has the lowest SIR_n and adding co-flow increases SIR_n hence increases the signal quality. We observe that the increment in SIR_n is not linear with the increment in co-flow. After $u_c = 0.01\,\text{m/s}$, doubling the co-flow increases SIR_n more compared to $u_c = 0.001\,\text{m/s}$ case. Another critical observation is about the ISI window length. We observe that the effect of ISI (by considering the change in SIR_n) becomes negligible after considering five previous emissions for the given system parameters. Please note that, this observation depends especially on T_s, if T_s is reduced to half then significant ISI would cover twice the number of symbol slots.

V. Conclusion and Future Work

In this paper, we investigated the non-linearity aspect of the turbulent diffusion channel for a sequential signal emissions. We demonstrated that the sequential molecular signals will be added together at the receiver linearly in a turbulent diffusion channel. We used different information sequence to distinguish each emission and also we considered the same information in all emissions to see their linearity effects in the receiver site. We also modeled the received molecular signal that includes ISI. Theoretical model utilizes a base of four signal types that includes the adequate information to model the received signal for sequential emission case. The analytical model enabled us to formulate the effect of ISI via SIR_n. Results and the empirical channel model showed that, the current emission is affected by a specific number of previous emissions (e.g., five for the considered parameters) and the interference effect of the earlier emissions are negligible. As a future study, we are aiming to investigate the molecular MIMO and see how different molecular signals will affect each other in lateral direction and explore the notions of spatial diversity.

References

[1] T. Nakano, A. W. Eckford, and T. Haraguchi, *Molecular Communication*, 1st ed. Cambridge University Press, 2013.

[2] J. Heidemann, M. Stojanovic, and M. Zorzi, "Underwater sensor networks: applications, advances and challenges," *Philosophical Transactions of Royal Society A*, vol. 370, no. 1958, pp. 158–175, 2012.

[3] N. Farsad, H. B. Yilmaz, A. Eckford, C.-B. Chae, and W. Guo, "A comprehensive survey of recent advancements in molecular communication," *IEEE Communications Surveys & Tutorials*, vol. 18, no. 3, pp. 1887–1919, 2016.

[4] M. Pierobon and I. F. Akyildiz, "Intersymbol and co-channel interference in diffusion-based molecular communication," in *IEEE International Conference on Communications (ICC)*, 2012, pp. 6126–6131.

[5] B. Tepekule, A. E. Pusane, H. B. Yilmaz, C.-B. Chae, and T. Tugcu, "ISI mitigation techniques in molecular communication," *IEEE Transactions on Molecular, Biological and Multi-Scale Communications*, vol. 1, no. 2, pp. 202–216, 2015.

[6] S. S. Assaf, S. Salehi, R. G. Cid-Fuentes, J. Sole-Pareta, and E. Alarcon, "Influence of neighboring absorbing receivers upon the inter-symbol interference in a diffusion-based molecular communication system," *Elsevier Nano Communication Networks*, vol. 14, pp. 40–47, 2017.

[7] W. Guo, T. Asyhari, N. Farsad, H. B. Yilmaz, B. Li, A. Eckford, and C.-B. Chae, "Molecular communications: channel model and physical layer techniques," *IEEE Wireless Communications*, vol. 23, no. 4, pp. 120–127, August 2016.

[8] H. ShahMohammadian, G. G. Messier, and S. Magierowski, "Optimum receiver for molecule shift keying modulation in diffusion-based molecular communication channels," *Nano Communication Networks*, vol. 3, no. 3, pp. 183–195, 2012.

[9] N. Garralda, I. Llatser, A. Cabellos-Aparicio, and M. Pierobon, "Simulation-based evaluation of the diffusion-based physical channel in molecular nanonetworks," in *IEEE Conference on Computer Communications Workshops*, 2011, pp. 443–448.

[10] B. D. Unluturk and I. F. Akyildiz, "An End-to-End Model of Plant Pheromone Channel for Long Range Molecular Communication," *IEEE Transactions on Nanobioscience*, 2017.
[11] N. Farsad, W. Guo, and A. W. Eckford, "Tabletop molecular communication: Text messages through chemical signals," *PloS one*, vol. 8, no. 12, p. e82935, 2013.
[12] I. Atthanayake, S. Esfahani, P. Denissenko, I. Guymer, P. Thomas, and W. Guo, "Experimental molecular communications in obstacle rich fluids," *Proc. ACM Int. Conf. on Nanoscale Comput. Commun. (NANOCOM)*, 2018.
[13] N. Farsad, N. Kim, A. Eckford, and C. Chae, "Channel and Noise Models for Nonlinear Molecular Communication Systems," *IEEE Journal on Selected Areas in Communications*, vol. 32, 2014.
[14] E. Kennedy, P. Shakya, M. Ozmen, C. Rose, and J. Rosenstein, "Spatiotemporal information preservation in turbulent vapor plumes," *Applied Physics Letters*, vol. 112, 2018.
[15] B. D. Unluturk and I. F. Akyildiz, "An end-to-end model of plant pheromone channel for long range molecular communication," *IEEE Transactions on Nanobioscience*, vol. 16, no. 1, pp. 11–20, 2017.
[16] P. J. Roberts and D. R. Webster, *Turbulent diffusion*. ASCE Press, Reston, Virginia, 2002.
[17] M. B. Jackson, *Molecular and cellular biophysics*. Cambridge University Press, 2006.